Enhanced Catalyst Durability and Sulfur Tolerance by Atomic Layer Deposition

Cooperative Research and Development Final Report

CRADA Number: CRD-18-00727

NREL Technical Contact: Derek Vardon

NREL is a national laboratory of the U.S. Department of Energy
Office of Energy Efficiency & Renewable Energy
Operated by the Alliance for Sustainable Energy, LLC

This report is available at no cost from the National Renewable Energy Laboratory (NREL) at www.nrel.gov/publications.

Contract No. DE-AC36-08GO28308

Technical Report
NREL/TP-5100-82242
February 2022

Enhanced Catalyst Durability and Sulfur Tolerance by Atomic Layer Deposition

Cooperative Research and Development Final Report

CRADA Number: CRD-18-00727

NREL Technical Contact: Derek Vardon

Suggested Citation
Vardon, Derek. 2022. *Enhanced Catalyst Durability and Sulfur Tolerance by Atomic Layer Deposition: Cooperative Research and Development Final Report, CRADA Number CRD-18-00727.* Golden, CO: National Renewable Energy Laboratory. NREL/TP-5100-82242. https://www.nrel.gov/docs/fy22osti/82242.pdf.

NREL is a national laboratory of the U.S. Department of Energy
Office of Energy Efficiency & Renewable Energy
Operated by the Alliance for Sustainable Energy, LLC

This report is available at no cost from the National Renewable Energy Laboratory (NREL) at www.nrel.gov/publications.

Contract No. DE-AC36-08GO28308

Technical Report
NREL/TP-5100-82242
February 2022

National Renewable Energy Laboratory
15013 Denver West Parkway
Golden, CO 80401
303-275-3000 • www.nrel.gov

NOTICE

This work was authored by the National Renewable Energy Laboratory, operated by Alliance for Sustainable Energy, LLC, for the U.S. Department of Energy (DOE) under Contract No. DE-AC36-08GO28308. Funding provided by U.S. Department of Energy Office of Energy Efficiency and Renewable Energy Bioenergy Technologies Office. The views expressed herein do not necessarily represent the views of the DOE or the U.S. Government.

This report is available at no cost from the National Renewable Energy Laboratory (NREL) at www.nrel.gov/publications.

U.S. Department of Energy (DOE) reports produced after 1991 and a growing number of pre-1991 documents are available free via www.OSTI.gov.

Cover Photos by Dennis Schroeder: (clockwise, left to right) NREL 51934, NREL 45897, NREL 42160, NREL 45891, NREL 48097, NREL 46526.

NREL prints on paper that contains recycled content.

Cooperative Research and Development Final Report

Report Date: February 17, 2022

In accordance with requirements set forth in the terms of the CRADA agreement, this document is the CRADA final report, including a list of subject inventions, to be forwarded to the DOE Office of Scientific and Technical Information as part of the commitment to the public to demonstrate results of federally funded research.

Parties to the Agreement: ALD NanoSolutions, Inc. (Currently known as Forge Nano); Johnson Matthey PLC

CRADA Number: CRD-18-00727

CRADA Title: Enhanced Catalyst Durability and Sulfur Tolerance by Atomic Layer Deposition

Responsible Technical Contact at Alliance/National Renewable Energy Laboratory (NREL):

Derek Vardon | derek.vardon@nrel.gov

Name and Email Address of POC at Company:

Karen Buechler | kbuechler@forgenano.com

Mike Watson | mike.watson@matthey.com

Sponsoring DOE Program Office(s):

Office of Energy Efficiency and Renewable Energy (EERE), Bioenergy Technologies Office (BETO)

Joint Work Statement Funding Table showing DOE commitment:

Estimated Costs	NREL Shared Resources a/k/a Government In-Kind
Year 1	$268,000.00
Year 2, Modification #1	$268,000.00
Year 3, Modification #2	$0.00
Year 4, Modification #3	$0.00
TOTALS	$536,000.00

Executive Summary of CRADA Work:

This CRADA advanced the use of atomic layer deposition (ALD) catalyst coatings to improve sulfur tolerance and demonstrate improved catalyst durability for biomass conversion chemistries. This project leveraged National Laboratory and industry expertise for ALD catalyst coating development between NREL, ALD NanoSolutions, Inc. ("ALD NanoSolutions"), and Johnson Matthey PLC ("Johnson Matthey"). To better understand the role of ALD coatings on catalyst activity and durability, a joint experimental and computational effort combined bench-scale ALD catalyst synthesis, material characterization, catalyst testing, and modeling of catalyst surface energetics. In addition, to demonstrate the commercial relevance of this technology, scaled ALD coated catalysts were subjected to continuous testing and accelerated aging to validate performance gains. Results were used to inform ALD catalyst coating manufacturing cost models, as well as biobased chemical process cost models.

Summary of Research Results:

Task 1: Deliver first suite of 8 ALD coated catalysts and report material characterization and durability testing results.

Three catalysts were delivered for the initial suite of ALD coated catalysts. These were used to examine the difference between an ALD overcoating approach (coating active metal and support) vs. ALD undercoating (coating the support before addition of the active metal). Physicochemical properties of the uncoated and ALD catalysts are reported in Table 1. The reduction in surface area and pore volume reflects the coverage of surface features and filling of pore void space on the support by the TiO_2 undercoating. The reduction in CO uptake, which is 7% and 68% for the 5c, where "c" refers to the number of ALD cycles, and 10c catalysts respectively, may be due to a reduction in Pd dispersion during synthesis or strong interactions between Pd and the TiO_2 undercoating that block CO adsorption sites.

Table 1. Physicochemical properties of uncoated and ALD coated catalysts.

Catalyst Description	Surface Area (m2 g-1)	Pore Vol. (mL g-1)	CO Uptake (µmol g-1)	Pd Loading (wt%)	Al or Ti (wt%)
Uncoated Pd/Al_2O_3	120	0.67	29.7	0.41	-
5c Pd/TiO_2-Al_2O_3	115	0.62	27.6	0.40	Ti 2.86
10c Pd/TiO_2-Al_2O_3	116	0.51	9.5	0.39	Ti 10.35
1c Al_2O_3-Pd/TiO_2	117	0.51	0	0.40	Al 2.84

The uncoated and ALD catalysts were screened for activity in batch muconate hydrogenation reactions before and after exposure to high temperature conditions (4 h at 700 °C in air followed by 4 h at 200 °C in H_2, Fig. 1). During reaction testing prior to thermal treatment, the undercoated Pd/TiO_2-Al_2O_3 catalysts exhibited productivity within ±3% of the baseline catalyst. This result demonstrates the potential of ALD undercoating as a tool for catalyst modification without major reductions in activity. Alternatively, more traditional ALD overcoating methods have the potential to restrict access to catalytic active sites, which is consistent with the comparatively low productivity of the overcoated Al_2O_3-Pd/TiO_2 catalyst reported here. After treatment at 700 °C, the productivity of all the catalysts increased. Enhancements ranged from 5-9% for the Pd/TiO_2-Al_2O_3 catalysts to >700% for the Al_2O_3-Pd/TiO_2 catalysts. In the former case, the increase may be due to thermally induced metal support interactions between Pd and TiO_2 that promote hydrogenation. In the latter case, the increase in productivity is attributed to thermal cracking of the Al_2O_3 coating, which has the potential to restore accessibility to the Pd active sites that were previously covered by the coatings.

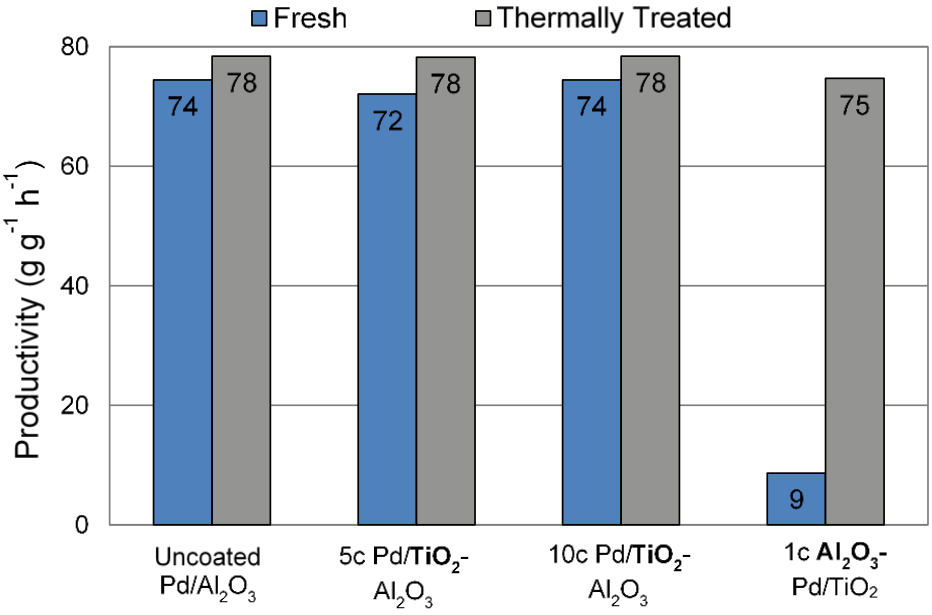

Fig. 1. Muconic acid conversion productivity reported as g muconic acid converted per g catalyst per min at 30 min time on stream for a series of uncoated and ALD-coated supported Pd catalysts before and after thermal treatments at 700 °C. Reaction conditions: 10 mg catalyst, 25 mL 2 wt% muconic acid in ethanol, 24°C, stirring at 1600 rpm.

The uncoated and ALD coated catalysts were screened for activity in batch muconate hydrogenation reactions in the presence and absence of cysteine, a biogenic sulfur compound. The amount of cysteine used for reactions was based on the nominal Pd loading and resulted in a S:Pd molar ratio of approximately 3:1. In all cases the introduction of sulfur decreased catalyst productivity (Fig. 2). For the uncoated Pd/Al_2O_3 and undercoated Pd/TiO_2-Al_2O_3 catalysts, the retention in productivity ranged from 14-42% and was generally proportional to the number of accessible Pd sites measured by CO chemisorption (Table 1). For the overcoated Al_2O_3-Pd/TiO_2, the retention in productivity was 30%. Although direct comparison across catalyst classes is confounded by differences in material properties and initial activity, these data suggest that the gravimetrically normalized sulfur tolerance is likely correlated with the density of Pd active sites and may be improved by increasing Pd dispersion.

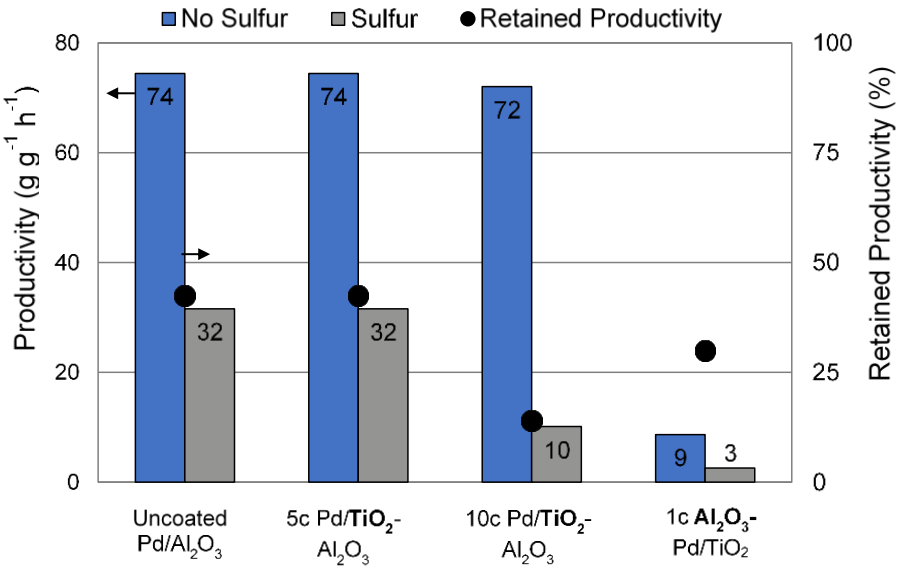

Fig. 2. Muconic acid conversion productivity reported as g muconic acid converted per g catalyst per min at 30 min of reaction for a series of uncoated and ALD-coated supported Pd catalysts with and without sulfur exposure during reaction. Retained productivity is relative to conversion observed by each catalyst in the absence of cysteine at 30 minutes of reaction. Reaction conditions: 10 mg catalyst, 25 mL 2 wt% muconic acid in ethanol, 24°C, stirring at 1600 rpm, spiked with 0.016 mg cysteine when indicated.

Task 2: Construct computational catalyst surface models with ALD coatings and report structure-S tolerance relationships for ALD catalyst coatings.

Rather than analyzing structure—S tolerance relationships, computational efforts were redirected to analyze the effects of a TiO_2 ALD coating on the adsorption of aromatic species such as naphthalene and tetralin on a Pd surface. The enhanced performance of $10cTiO_2$-Pd/Al_2O_3 catalyst, as detailed in Task 3-4, was the impetus for this shift. Density functional theory (DFT) calculations were performed through the Vienna Ab initio Simulation Package (VASP). In particular, three different models were considered: (i) a bare Pd(111) surface ("Bare Pd") to capture the role of un-coated Pd catalysts, as well as (ii) complete ("OH-TiO_2/Pd") and (iii) truncated ("tOH-TiO_2/Pd") rutile-TiO_2(110) overlayers to capture the role of complete and partial coverage of the Pd catalyst by the TiO_2 overcoat, respectively. For the two models containing rutile-TiO_2, we terminated the overlayer with OH groups as hydrogenation of the surface oxygen anions is expected to readily occur in the presence of H_2 during naphthalene hydrogenation. Representative structures for each surface are shown in Fig. 3(a).

The main work from our computational analyses focused on calculating the adsorption strength for key surface intermediates in both naphthalene hydrogenation and CO uptake studies: namely, H, H_2, CO, and naphthalene. These adsorption energies were calculated for each species on the three surfaces studied and are provided in Fig. 3(b). Relative to the bare Pd(111) surface, the presence of a full rutile-TiO_2 overcoat significantly destabilizes adsorption by 2.79 eV, 0.23 eV, 1.93 eV, and 2.06 eV for H, H_2, CO, and naphthalene, respectively (1 eV = 96.5 kJ/mol). These results suggest that the presence of a full rutile-TiO_2 overlayer will significantly reduce the surface coverage of CO, as well as reduce hydrogen activation and availability for hydrogenation reactions.

When we switch to a truncated rutile-TiO_2 overlayer, we find that the adsorption energy for the smaller adsorbates studied (i.e., H, H_2, and CO) are stabilized relative to the bare Pd(111) surface by 0.03 eV for H, 0.88 eV for H_2, and 0.25 eV for CO. The adsorption energy for naphthalene, however, remains destabilized by 2.07 eV relative to the bare Pd(111) surface. Because the adsorption strength of H remains high and H_2 dissociates upon adsorption, the presence of this truncated overlayer does not impact either hydrogen activation or surface accumulation, which are both crucial to high hydrogenation activities. In addition, the stabilization of CO helps explain the observed drop in CO uptake with the application of the ALD layer to Pd/Al_2O_3, as the decrease can be largely attributed to Pd-site blocking by partial TiO_2 overlayers and not CO destabilization. Lastly, because naphthalene is still largely destabilized due to its inability to access Pd binding sites, this leaves these Pd sites free for hydrogen activation and which may help to explain the observed increase in naphthalene hydrogenation activity in the presence of TiO_2 overcoats.

Furthermore, to explain why the adsorption of H, H_2, and CO were stabilized in the presence of a partial rutile-TiO_2 overlayer versus the bare Pd(111) surface, we compared the average surface charge of Pd in each of the three systems studied. These results are presented in Fig. 3(c). We find that when a rutile-TiO_2 overlayer is present, it donates charge to the Pd surface and results in a partially negative-charged surface. This negative charge helps to explain the stabilization of these three surface intermediates, as H and C (the atom through which CO binds to the surface) are reasonably electronegative.

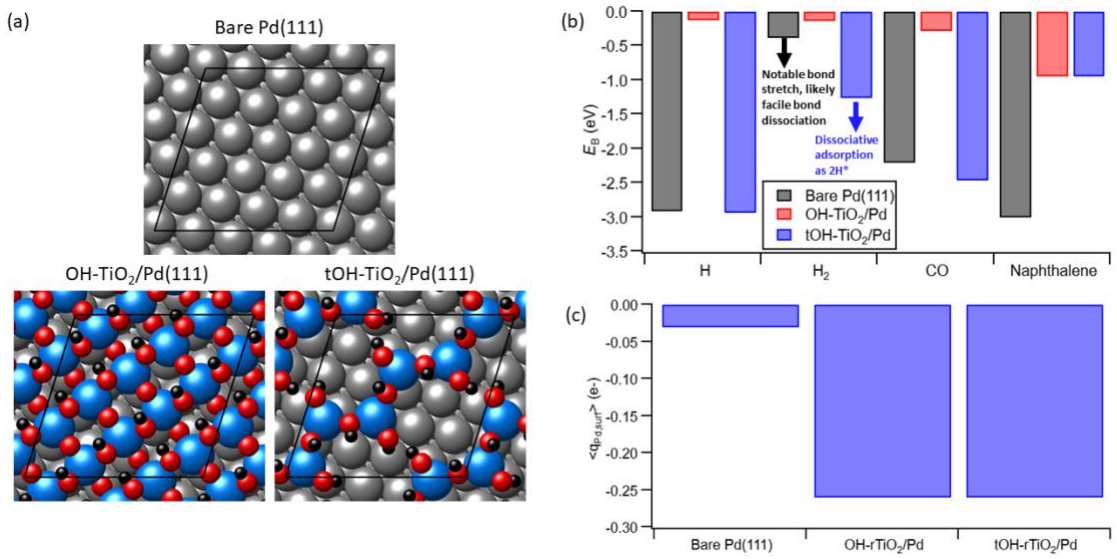

Fig. 3. (a) Top views of the three surfaces considered in the DFT studies: the bare Pd(111) surface ("Bare Pd(111)"), a full OH-terminated rutile-TiO_2 overlayer on Pd(111) ("OH-TiO_2/Pd(111)"), and a truncated OH-terminated rutile-TiO_2 overlayer on Pd(111) ("tOH-TiO_2/Pd(111)"). Atom colors: grey – Pd, blue – Ti, red – O, and black – H. (b) Adsorption energies (E_B, in eV; 1 eV = 96.5 kJ/mol) for H, H_2, CO, and naphthalene on the Bare Pd(111) (black bars), OH-TiO_2/Pd(111) (red bars) and tOH-TiO_2/Pd(111) (blue bars) surfaces. E_B is calculated as $E_B = E_{tot} - E_{clean} - E_{gas}$, where E_{tot} is the total energy of the adsorbate+surface complex, E_{clean} is the total energy of the clean surface, and E_{gas} is the total energy of the adsorbate in the gas phase. (c) Average charge of the Pd surf ($<q_{Pd,surf}>$, in units of electron charge) in the three systems shown in (a). Atomic charges were calculated using Bader charge analysis.

Task 3: Deliver second suite of 8 ALD coated catalysts that incorporate initial experimental and computational findings, and report material characterization and durability testing results.

A second suite of nine ALD coated catalysts was delivered using Al_2O_3 and TiO_2 overcoats on both Pd/TiO_2 and Pd/Al_2O_3 base catalysts. Thermal stability was probed using XRD to assess the phase and composition of all catalysts before and after treatment at 700 °C. XRD data from the thermally treated Pd/TiO_2 catalyst (Fig. 4a) showed evidence of peak narrowing for anatase TiO_2 diffractions, which is attributed to phase restructuring. This process is associated with pore collapse and a loss of support surface area. Similar restructuring was observed after thermal treatment of the TiO_2-coated Pd/TiO_2 catalyst. In contrast, the Al_2O_3-coated Pd/TiO_2 catalysts exhibited increased resistance to thermal restructuring, with no evidence of morphological changes to TiO_2 when at least 1 full ALD cycle was applied. Unlike the uncoated Pd/TiO_2 catalysts, the XRD data provided no evidence of thermally induced changes to the uncoated Pd/Al_2O_3 catalyst (Fig 4b) at the temperatures utilized in these experiments. However, data from the 10c TiO_2-Pd/Al_2O_3 catalyst depicted the presence of anatase TiO_2. This result is attributed to crystallization of the amorphous TiO_2 ALD coating during thermal treatment and provides evidence that these methods can be utilized for targeted catalyst modification to achieve highly structured metal TiO_2 phases that have the potential to improve sulfur tolerance (*vida infra*).

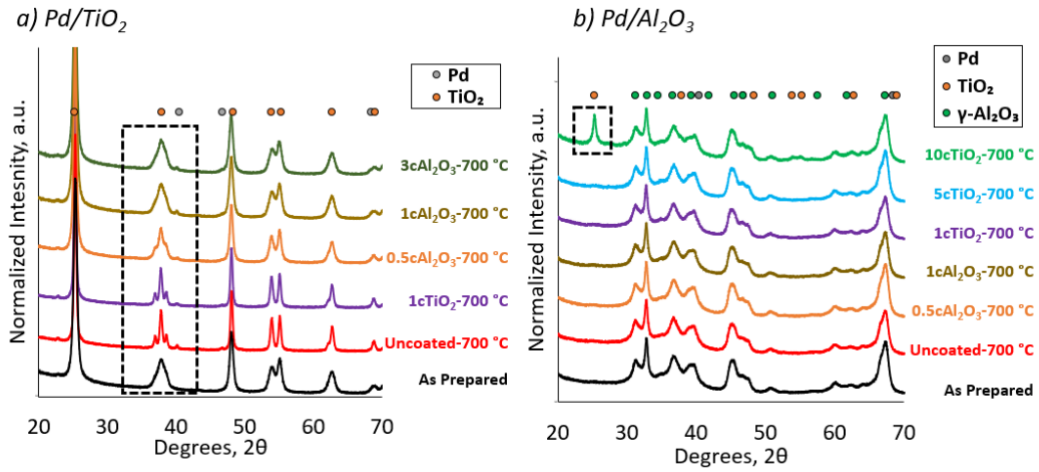

Fig. 4. XRD data for a series of uncoated and ALD-coated a) Pd/TiO_2 and b) Pd/Al_2O_3 catalysts before and after thermal treatments at 700 °C.

Sulfur tolerance was probed using batch naphthalene hydrogenation reactions performed in the presence and absence of DMDS. Naphthalene hydrogenation was chosen over muconic acid hydrogenation due to its more conventional usage as a S poisoning probe reaction, as well to assess the effects of the ALD coatings on aromatic hydrogenation. The amount of DMDS used for reactions was based on the nominal Pd loading and resulted in a S:Pd molar ratio of approximately 1:5. As shown in Fig. 5, the introduction of sulfur resulted in a ca. 70-80% reduction in productivity on the uncoated Pd/TiO_2 and Pd/Al_2O_3 catalysts, which is attributed to poisoning of active sites by strongly-bound atomic sulfur (Fig 3a). In all cases, the ALD catalysts exhibited improved stability against sulfur poisoning compared to the uncoated catalysts. The highest productivity in the presence of sulfur was observed over the TiO_2-coated materials. The performance of the 10c TiO_2-Pd/Al_2O_3 catalyst was particularly noteworthy in that it exhibited productivity values higher than the uncoated Pd/Al_2O_3 in the presence and absence of sulfur.

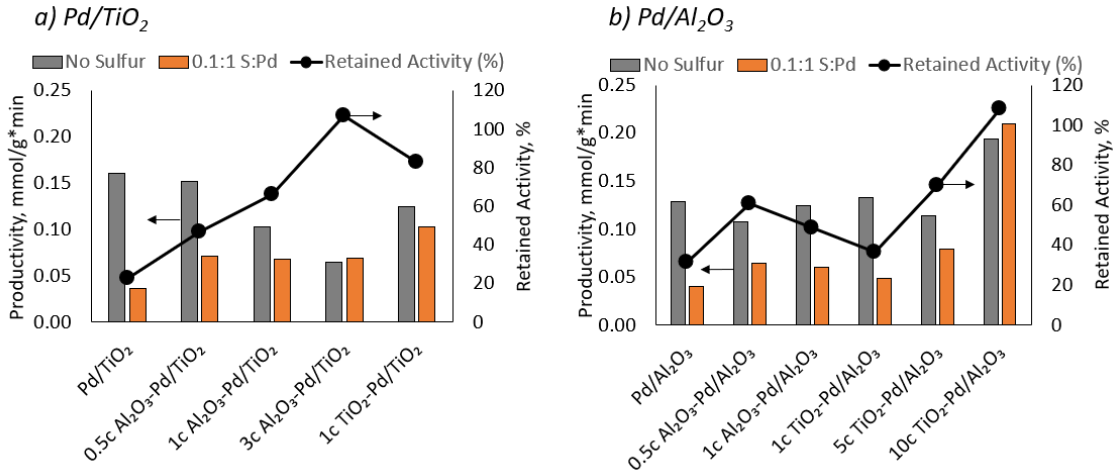

Fig. 5. Naphthalene conversion productivity for a series of uncoated and ALD-coated a) Pd/TiO_2 and b) Pd/Al_2O_3 catalysts with and without sulfur exposure. Retained productivity is relative to conversion observed by each catalyst in the absence of DMDS. Reaction conditions: 25 mg catalyst, 10 mL 1 wt% naphthalene in tridecane, 200 °C, stirring at 1200 rpm, 40 bar hydrogen, 75 min exposure.

Task 4: Down-select at least 1 ALD catalyst to synthesize at the 1-kg scale and report the 24-h time on stream performance for muconic acid hydrogenation in the absence and presence of trace sulfur.

The 10cTiO_2-Pd/Al_2O_3 catalyst was down-selected and synthesized at the 100-g scale, rather than 1-kg, based on feedback that sufficient ALD synthesis and catalyst performance information could be obtained at this scale. The ALD recipe for the down-selected 10cTiO_2 catalyst was scaled from its original 3 g batch size (label T414a) to a 100 g batch size and synthesized in triplicate by Forge Nano (labels T438a, T439a, and FN0381). The 100 g samples were characterized by physisorption, chemisorption, and naphthalene hydrogenation screening in batch reactors (Table 2 and Fig. 6). BET surface area and H monolayer uptake were found to be slightly higher for the 100 g samples than the original 10cTiO_2 material. The ALD recipe was modified slightly during the scale-up, leading to an expected elemental content of approximately 7 wt% Ti on the 100 g batches (based on ICP-OES analysis of a trial batch synthesized at intermediate scale, not pictured) as opposed to the recorded 9 wt% Ti on the original T414a. This modified deposition may have resulted in higher physical and metal surface areas on the coated 100 g catalyst batches. When examined for naphthalene hydrogenation, the scaled catalysts were found to have similar tetralin productivities to T414a, with batches 439a and FN0381 even exceeding T414a. All catalysts coated with the scaled ALD recipe were more active than the base Pd/Al_2O_3 material, indicating the observed activity benefits of TiO_2 ALD can be retained upon scale-up. Performing ALD onto very high surface area particles poses unique scale-up challenges. T439a and FN0381 are quite similar in performance and physical characteristics. The early-stage trials seen here demonstrate the ability to provide this coating at very large scale on high surface area catalyst particles.

Table 2. Physisorption and chemisorption characterization of down-selected ALD catalyst at different ALD-coating synthesis scales.

Catalyst Sample	BET surface area (m2 g-1)	H monolayer uptake (μmol g-1)
10cTiO2 (T414a, 3 g)	110	10.5
10cTiO2 (T438a, 100 g)	116	24.5
10cTiO2 (T439a, 100 g)	122	24.0
10cTiO2 (FN0381, 100 g)	122	18.1

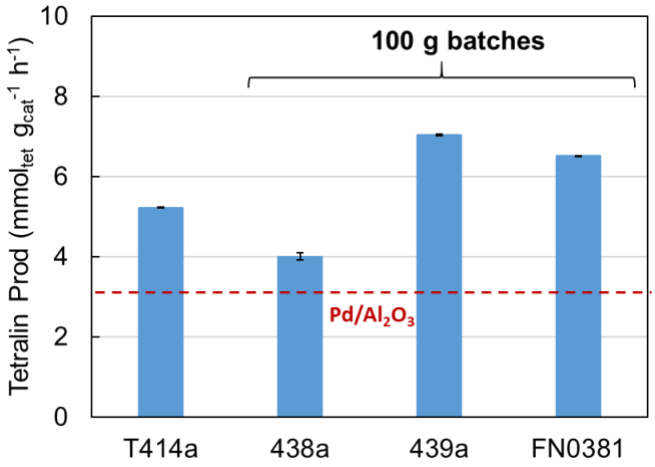

Fig. 6. Batch reactor tetralin productivity of down-selected ALD catalyst at different synthesis scales. Batch reactor conditions: 10 mL of 1 wt% naphthalene reactant in tridecane solvent with 0.5 wt% pentadecane surrogate; 25 mg catalyst; 200°C; 40 bar H_2; 180 min; 800 rpm.

Naphthalene hydrogenation was kept as the probe reaction of choice and sulfur was excluded from time on stream testing due to concerns over reactor contamination. The 10cTiO$_2$-Pd/Al$_2$O$_3$ catalyst was tested against uncoated Pd/Al$_2$O$_3$ and Pd/TiO$_2$ for 8 h at partial conversion, with the first 2 h excluded for reaction stabilization. The results of these tests are shown in Fig 7. As seen in batch screening, the 10cTiO$_2$ catalyst outperformed the uncoated controls. When normalized by bulk Pd content, 10cTiO$_2$ had ~1.7X the steady-state tetralin productivity of Pd/Al$_2$O$_3$, which provides evidence that the hydrogenation rate enhancement of the ALD coating is also present in flow conditions. The superior performance of 10cTiO$_2$ was maintained over the course of the 8-h experiment, indicating that the ALD coating may improve the stability of the Pd/Al$_2$O$_3$ catalyst.

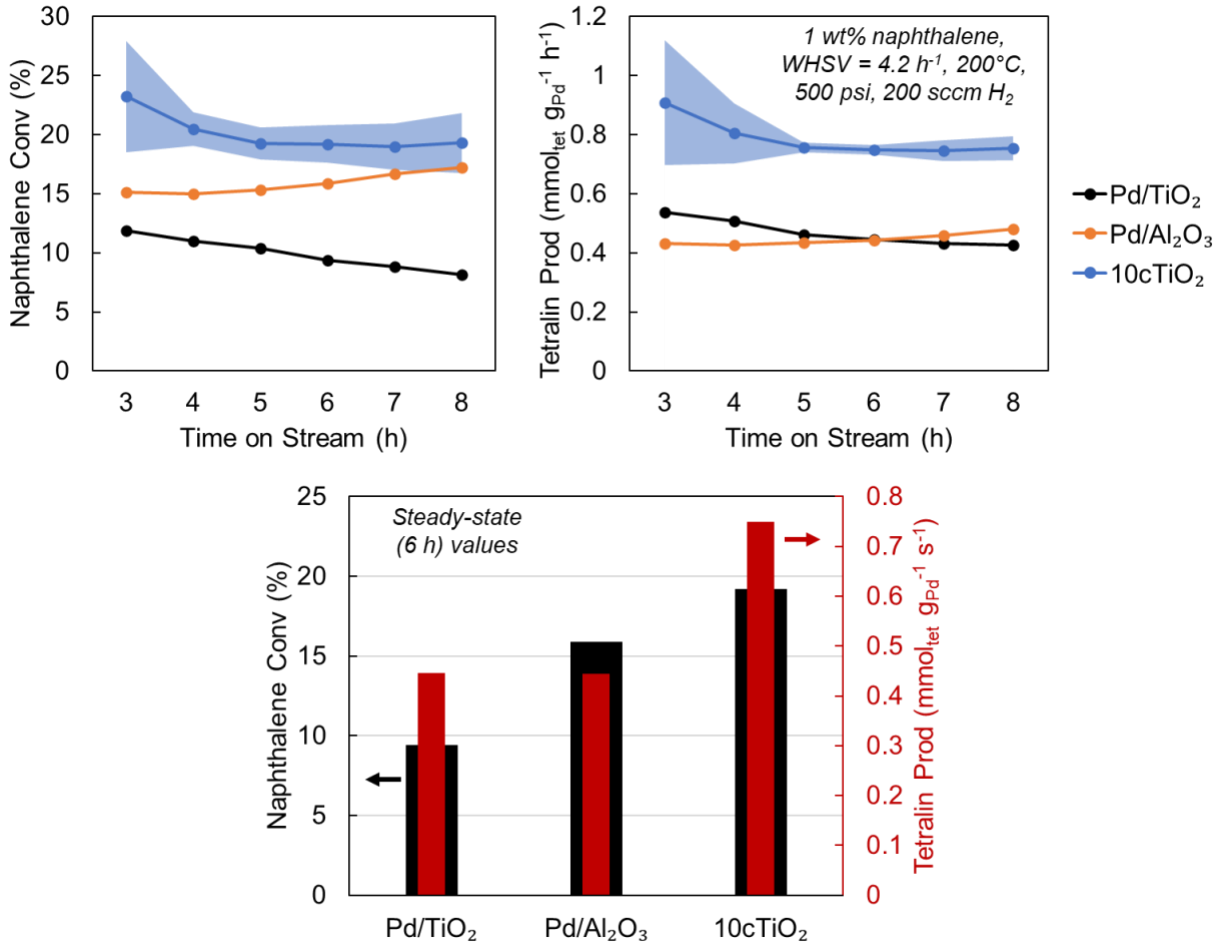

Fig. 7. Naphthalene molar conversion and Pd-normalized tetralin productivity of down-selected ALD catalyst ($10cTiO_2$) compared to Pd/Al_2O_3 and Pd/TiO_2 in flow reactor experiments. Conversion and productivity at steady-state (6 h) are also directly compared in the bar plot below. Note that $10cTiO_2$ was run in duplicate and the shaded region represents standard deviation between experiments. Flow reactor conditions: 1 wt% naphthalene reactant in tridecane solvent with 0.5 wt% pentadecane surrogate; 1 mL min^{-1} pump speed; 200 sccm H_2; 0.1 g catalyst; WHSV = 4.2 h^{-1}; 200°C; 500 psi H_2; 1 h sampling intervals.

Task 5: Deliver techno-economic cost models for (i) manufacturing ALD catalyst coatings, and (ii) producing biobased adipic acid via muconic acid hydrogenation with ALD coated catalysts.

In addition to pursuing advancements in ALD-enabled catalyst performance, a longstanding goal of our research has been to identify quantitative and qualitative insights on the factors that make ALD coatings cost-effective. In Fig. 8, we present a number of these factors and assess the ALD inputs or outcomes that would result in the coating being cost-prohibitive (red), borderline (orange), or cost-effective (green). The factors include catalyst activity and selectivity, degradation resistance, and suitability for end-of-life metals reclamation. Dotted green boxes denote our previous achievements of ALD coatings that appear to be cost-effective, while solid green boxes indicate favorable cost-benefit characteristics achieved in this project. Of course, it is rare to see change in one of these categories without any change in the others; see below for a more detailed exploration of the various factors.

For this project, we found that the 10cTiO_2 catalyst has an excellent case for cost effectiveness, with $22/kg catalyst or more of net benefit and an estimated coating cost of only $12/kg (see below for more details). The important factors leading to a cost-effective coating are the 1.7X activity improvement with the coating, a titania precursor (TTIP) price of ca. $5/kg, and a production scale of >10 tonnes/day (a scale that will soon be available at Forge Nano). A decreased production scale would increase not only production costs but also the precursor price because of volume-dependent pricing; therefore, a key insight for this catalyst is that achieving sufficient scale to cut production costs and obtain a TTIP price below $10/kg is essential. If an improvement in catalyst lifetime could be demonstrated or if it were possible to obtain similar benefits with fewer ALD cycles, the value proposition of the ALD coating would only improve. This analysis will be employed as we continue to study the pathway to commercialization of ALD-coated catalysts and to pursue qualitative and quantitative milestones that can guide research and development efforts.

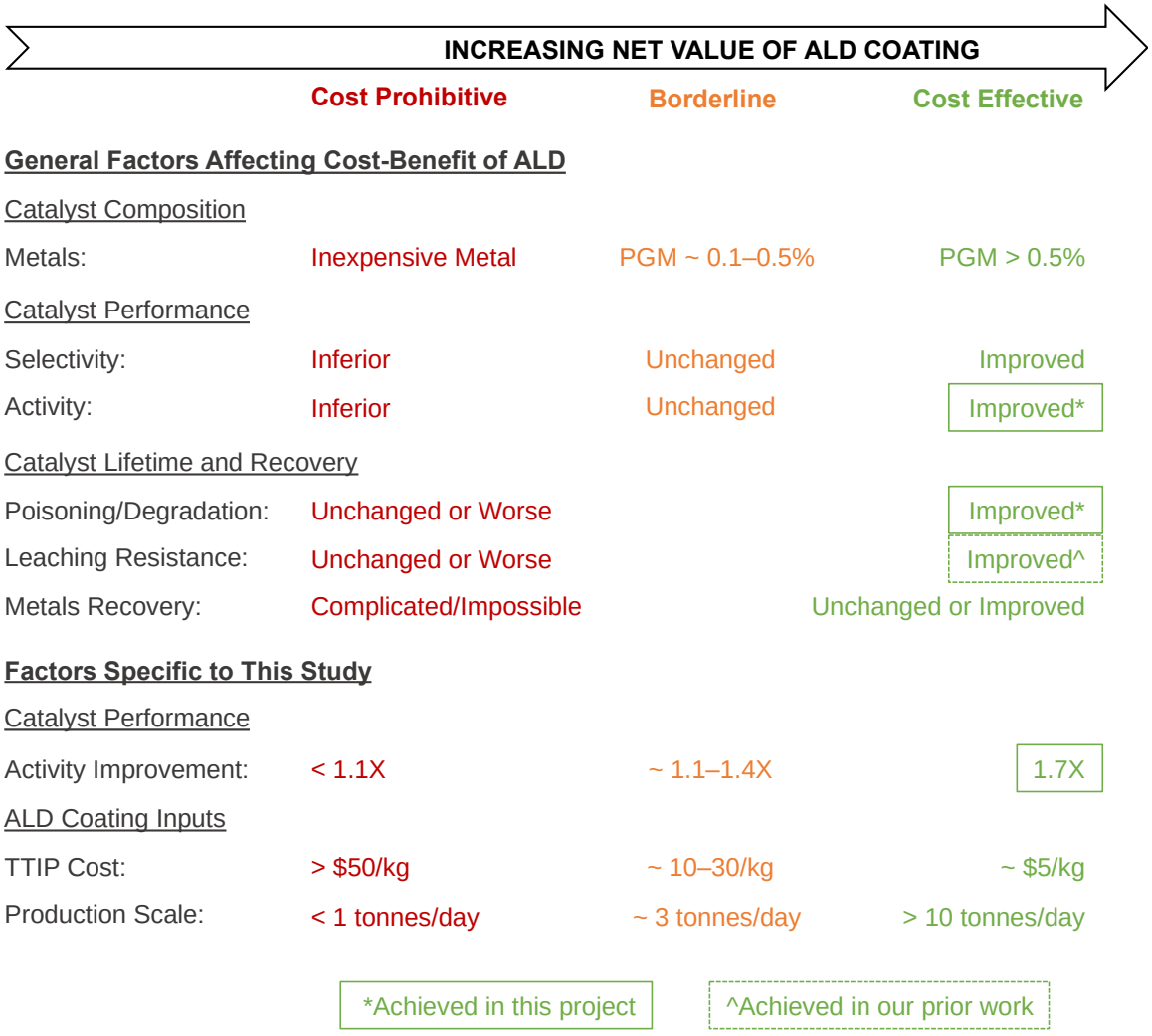

Fig 8. Value provided by ALD coating catalysts relevant to composition, performance, and lifetime.

The value proposition of the ALD coatings (Fig. 8) was assessed through a techno-economic analysis performed by Forge Nano and NREL. In keeping with our experimental findings, this techno-economic analysis was performed in the context of aromatic hydrogenation, rather than muconic acid hydrogenation. We sought to determine whether the observed performance improvement for $10cTiO_2$ compared to the baseline Pd/Al_2O_3 yielded sufficient savings to justify the added cost of the ALD coating. Since lifetime is challenging to assess and, at a minimum, $10cTiO_2$ appears more durable than uncoated Pd/Al_2O_3 (see above), we assumed the ALD coating did not change catalyst lifetime. The economic benefit of the increased catalyst activity reported above is a corresponding reduction in the required catalyst loading. A Cat Cost estimate for the 0.44% Pd/Al_2O_3 catalyst at 200-tonne order size produced a purchase cost of $177/kg and a net cost, including spent catalyst value, of $54/kg. The reduced catalyst loading possible with $10cTiO_2$ therefore corresponds to a net cost savings of $54 – $54/1.7 = $22 per kg of the baseline Pd/Al_2O_3 catalyst ($73/kg savings in purchase cost). This net cost savings represents the ALD coating cost needed to provide a net benefit from solely a catalyst material cost standpoint. The use of a more active ALD coated catalyst also allows for equipment capital savings for hydrogenation chemistry. For example, when applied to a small-scale refinery processing 75,000 barrels per day (mass flow rate of 422,000 kg/h, WHSV 2 h^{-1}, catalyst loading 211 tonnes), increasing the catalyst activity by 1.7x results in an installed reactor capital cost savings of 45% due to reduced catalyst material loading requirements, which equates to over $22MM at this process scale. Likewise, operational savings may be realized with a more active catalyst through lower operating temperatures, which can further improve hydrogenation yields through improved liquid phase hydrogen solubility and hydrogenation equilibrium.

Modeling of the ALD coating cost was performed using Forge Nano data and is reported per kg of Pd/Al_2O_3 catalyst prior to coating, for simplicity. The cost model assumed two parallel trains of the Forge Nano Morpheus semi-continuous process operating at scale as a toll manufacturing service rather than an in-house ALD unit at a catalyst producer, with commodity-scale ALD precursor prices and process rates assumed for catalyst coating. A titanium isopropoxide (TTIP) precursor price of $5/kg was used with precursor recycle during ALD coating and a coating scale of 30 tonne of catalyst per day for a 200-tonne catalyst order. This results in an ALD coating cost of $12 per kg of catalyst, well below the $22 per kg savings in net catalyst costs (including Pd reclamation using CatCost) and provides 28% savings in catalyst material costs from increased activity with ALD coating. At the process scale of 211 tonnes of hydrogenation catalyst loading, this saves $5.4MM in material costs. Furthermore, it should be noted that beyond simple cost savings, reducing catalyst loading enabled by ALD can have significant process intensification benefits, allowing the use of smaller and more energy-efficient reactors.

To assess ALD-coating costs en route to scale-up, sensitivity analysis was performed at lower process scales and higher TTIP precursor costs. The factor with the greatest influence on coating cost is the TTIP precursor cost, as shown in Table 3. Increasing the TTIP price by 5x to $25/kg resulted in nearly a 4x increase in ALD coating cost ($43.84/kg catalyst), as the ALD coating precursor is the primary operational expense. As such, increasing the TTIP production scale to commodity levels and incorporating ALD precursor recycle during ALD coating manufacturing are essential to achieving cost reductions. Reducing the ALD coating equipment capacity by 2-fold resulted in a minor increase of $1.39/kg, highlighting the minimal impact of capital cost at this coating scale. Lastly, within the context of the 15 tonne/day production scale, order size had only a small effect on coating cost which indicates that per-run costs, such as cleaning supplies and labor, changeover downtime, and maintenance, are relatively minor at this production scale.

Table 3. Influence of TTIP precursor price and ALD coating equipment capacity on the total ALD coating cost for 1 kg of catalyst.

TTIP Precursor Price ($/kg)	Equipment Capacity (tonnes/day)	ALD Coating Cost ($/kg catalyst)
5	30	$12.08
5	15	$13.47
10	15	$20.67
10	3	$29.64
25	30	$43.84

Conclusions

In conclusion, this report provides a summary of work to date on the development of a highly active, durable, and S tolerant hydrogenation catalyst synthesized via TiO_2 ALD overcoating. The Pd/Al_2O_3 catalyst with 10 cycles of TiO_2 ALD applied was found to have superior performance in batch and flow hydrogenation testing when compared to uncoated catalysts. ALD catalysts synthesized at the 100-g scale showed similar hydrogenation activity to those synthesized at the 3-g scale, indicating that this powder catalyst ALD coating process can be scaled by 2-orders or magnitude without causing significant changes in final material properties. Computational techniques were utilized to probe the origin of the ALD-coated catalyst's enhanced hydrogenation activity and examine the effects of the TiO_2 overlayer on surface adsorption processes. Finally, the techno-economic model for TiO_2 ALD-coated catalysts confirmed the value proposition at commodity manufacturing scale, while helping to clarify the path to commercial viability for ALD-coated catalysts more generally. Due to increased catalyst activity with ALD coating, catalyst material cost savings of 28% and hydrogenation reactor capital saving of 45% may be realized.

Subject Inventions Listing:

Catalysts, Catalyst Supports and Methods of Making the Same. U.S. Provisional Patent Application No. 62/720,444, Vardon, D.R., Christensen, S.T., Hurst, K.E., Settle, A.E., Griffin, M.B.; Filed August 21, 2018, Expired August 25, 2019.

Catalysts, Catalyst Supports and Methods of Making the Same. U.S. Non-Provisional Patent Application No. 16/535,674, Vardon, D.R., Christensen, S.T., Hurst, K.E., Settle, A.E., Griffin, M.B., Filed August 08, 2019, Issued October 20, 2021 as U.S. Patent No. 11,167,281.

ROI #:

NREL ROI 18-109. *ALD coatings for metal oxide catalyst support.* Vardon, D.R., Christensen, S.T., Hurst, K.E., Settle, A.E., Griffin, M.B.